ELSEVIER

Journal of Nuclear Materials 296 (2001) 165–173

journal of nuclear materials

www.elsevier.com/locate/jnucmat

Retention of implanted hydrogen and helium in martensitic stainless steels and their effects on mechanical properties

P. Jung *, C. Liu, J. Chen

Institut für Festkörperforschung, Forschungszentrum Jülich, Association EURATOM-FZJ, Jülich D-52425, Germany

Abstract

Martensitic stainless steels are candidate materials for the target structure of the European Spallation Source (ESS). Hydrogen and helium produced by nuclear transmutation in the proton beam and in the energetic neutron field cause changes of material properties in addition to those caused by atomic displacement. The present work presents results of diffusion and retention of hydrogen and helium, derived from permeation and thermal desorption experiments. Furthermore synergy effects are discussed which occur when hydrogen is retained due to the presence of helium. Measurements of the effect of hydrogen and helium on hardness and tensile properties are given and results on fracture, creep rupture and fatigue are reviewed.

1. Introduction

Martensitic stainless steels are candidates for structural materials in future high-power spallation neutron sources as well as in fusion reactors. In comparison to austenitic stainless steels, this class of materials is favourable due to their higher mechanical strength and their lower susceptibility to void swelling, irradiation creep and high temperature helium embrittlement. On the other hand, points of concern are possible problems with welding, irradiation-induced embrittlement at low temperatures and embrittlement by hydrogen due to its lower solubility. Only recently in the fusion material programme, an increase of the ductile-to-brittle transition temperature (DBTT) by helium has also been observed. This means that effects of the light transmutation elements hydrogen and helium, which in a spallation source are produced in even larger amounts than in a fusion reactor, deserve more investigation. In the past, several martensitic stainless steels have been developed in the fast breeder and fusion reactor programs, showing that chromium concentrations around 9% are a good compromise between the better corrosion resistance of higher Cr-steels and the lower irradiation embrittlement of lower Cr-steels. In the following, results are mainly presented for three martensitic steels with different chromium content, the compositions of which are given in Table 1.

The production rates of H- and He-isotopes by nuclear reactions induced by neutrons and protons have been discussed in great detail during the present workshop. A compilation of experimental data [1,2] is given in Fig. 1, including some model calculations [3,4]. A typical value for He production in the European Spallation Source (ESS) window is estimated to $\approx$0.3 at.ppb/s, while the production in the containment and in the moderator is lower by a factor of 60. On the other hand, the production rate for hydrogen in the window is about a factor of 20 higher than for He.

As long as no powerful source of high-energy protons and spallation neutrons is available, the production of hydrogen and helium in materials must be simulated by implantation of particle beams. Other methods like isotope tayloring for reactor irradiation – e.g., helium production by adding ^{59}Ni or ^{10}B – have strong drawbacks by altering the properties of the base material in an unacceptable way [5]. By implantation rather large concentrations of H or He can be introduced with relatively low simultaneous defect production. This allows to study the almost 'pure' effect of these atoms but, on the other hand, means that the

* Corresponding author. Tel.: +49-2461 614 036; fax: +49-2461 614 413.

E-mail address: p.jung@fz-juelich.de (P. Jung).

0022-3115/01/$ - see front matter
PII: S0022-3115(01)00545-1

Table 1
Main constituents of some 7–12% Cr martensitic steels

	Fe	Cr	W	V	Ta	Mn	C	N
F82H	89.8	7.7	1.94	0.16	–	0.16	0.09	0.006
EUROFER97	89.1	9.0	1.1	0.20	0.075	0.40	0.11	0.03
MANET-II	86.3	10.3	–	0.2	Nb:0.12	0.79	0.10	0.024

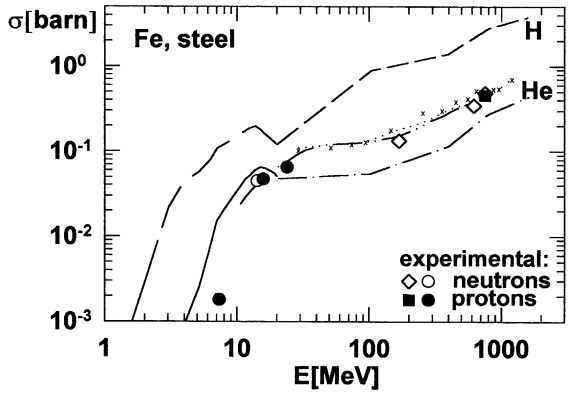

Fig. 1. Experimental production cross-section for ^{4}He by protons (●■) [1,2] and neutrons (○◇) cf. Ref. [3,4] as a function of energy. Included are calculations for Fe(p, He) with DIDACS (xxx), for Fe(n, He) with DIDACS (.....) and with DISCA2 [3] (-..-), and for SS316(n,He) (__, -.-) and SS316(n, H) (__, --) with SPECTER and LAHET [4].

situation in a spallation or fusion environment is not perfectly simulated.

2. Diffusion and retention of hydrogen

The main sources of hydrogen in the target area of a liquid metal spallation source are $(p, p'x)$ and (n, px) transmutation reactions of the primary protons. Another possible source could be absorption of hydrogen which might be added as a corrosion inhibitor. Only in the second case a diffusion barrier would be beneficial in reducing the hydrogen content of the metal, while hydrogen produced by transmutation would be effectively retained by barriers and hydrogen content would be linearly increasing with time and production rate G_H. The same would happen if diffusion coefficient D would be negligible at low temperatures or due to trapping. A critical concentration c^* for hydrogen embrittlement, estimated at about 10 wt.ppm in 10% Cr steels [6], would thus be reached in the ESS window ($G_H \approx 6 \times 10^{-9}$ s^{-1}) within about 26 h. This indicates that diffusion barriers are not desirable, but actually must be carefully avoided. Straightforward calculations for a slab of thickness d with one surface permeable and one sealed give a stationary maximum concentration of $c_{max} = d^2 \times G_H/2D$, while for both surfaces permeable the value would be a factor of 4 lower. From these expressions maximum values of d or minimum values of D (and thus also of temperature) can be derived if c^* is used for c_{max} [6,7].

Several techniques can be used to measure diffusion of hydrogen in solids as reviewed in [8]. In the present study, the effect of irradiation has been taken into account by performing permeation measurements during implantation and thermal desorption measurements after implantation [9]. Fig. 2 shows effective diffusion coefficients D^* of hydrogen in martensitic stainless steels as derived from transients in gas permeation experiments [10,11]. At temperatures above about 350°C, D^* of steels parallels the values in pure iron, while at lower temperatures it increasingly drops below the iron values due to trapping. In martensitic stainless steels, this effect is systematically enhanced with increasing chromium content. Also irradiation damage is reducing D^*, mainly at low temperatures [10,11]. On the other hand the effective binding energy to traps, as derived in the frame of an 'unsaturable trap model', is not significantly changed

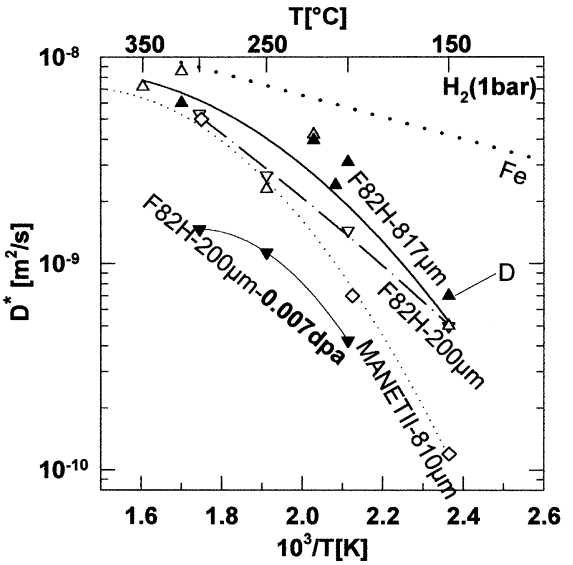

Fig. 2. Diffusion of hydrogen (and deuterium ▲) in unirradiated F82H and after irradiation to 0.007 dpa derived from permeation transients [10]. Specimen thickness is indicated. Included are results for MANET-II [11] and pure iron [12].

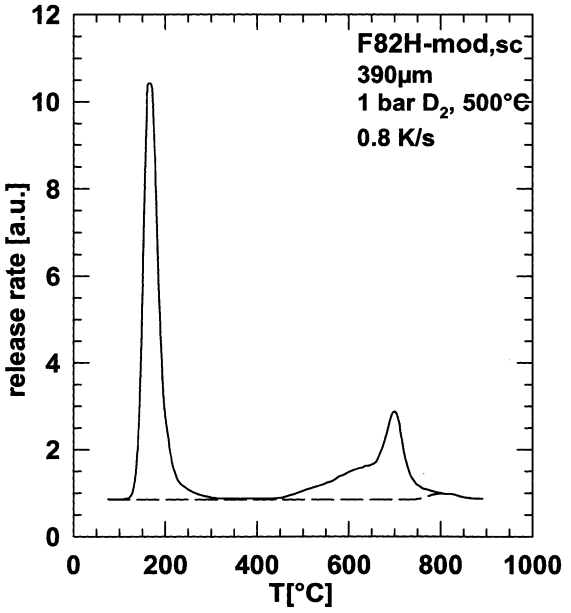

Fig. 3. Thermal desorption rates of deuterium as a function of temperature from 390 μm thick F82H specimens, thermally loaded at 1 bar and 500°C. The specimens were linearly heated at a rate of about 0.8 K/s. Similar behaviour is observed for virgin and pre-irradiated specimens [9].

by irradiation, indicating that in both cases essentially the same traps are acting. This is corroborated by the similarity of thermal desorption behaviour of specimens loaded with deuterium in the virgin state and after irradiation (Fig. 3). In both cases, two prominent peaks are observed around 200°C and 700°C, the precise positions depending on heating rate and specimen thickness.

3. Diffusion and retention of helium

As helium is virtually insoluble in metals, it is produced in materials of spallation sources or fusion reactors practically only by transmutation reactions. A much weaker source of He is decay of dissolved tritium (from transmutations) to ^{3}He. Helium is readily immobilised by trapping (for example in vacancies) or clustering and is therefore quantitatively retained. This means that for a production rate G_{He} of 3×10^{-10} s^{-1} (ESS window) a concentration of 100 at.ppm is reached already within 4 days. Critical concentrations in this range have been established for high-temperature helium embrittlement in austenitic stainless steels [13], while even smaller values seemingly cause increases of DBTT in martensitic steels [14,15]. Diffusion coefficients as well as concentration limits for immobilisation by clustering of helium have been obtained in iron from thermal desorption measurements at very low implanted helium concentrations in very thin specimens. The relative amounts released during linear and isothermal heating strongly depend on specimens thickness d and initial helium concentration c_0 as shown for iron in Figs. 4 and 5. For significant desorption by free diffusion, as indicated by a square root time dependence in Fig. 5, the product $d\sqrt{c_0}$ must not significantly exceed $\sqrt{(\Omega/2R)}$, where Ω and R are atomic volume and interaction radius of the helium atoms, respectively [16]. In the ESS window, with the above value of G_{He} this limit is exceeded within a few minutes. After that time helium is practically quantitatively retained.

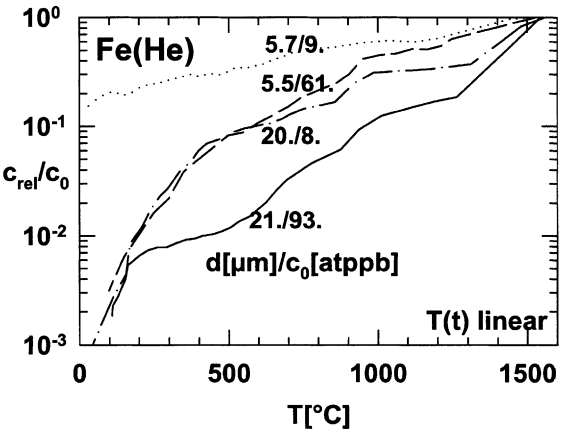

Fig. 4. He release from implanted iron during linear heating at a rate of about 0.8 K/s. The numbers give specimen thickness and initial He concentration [16].

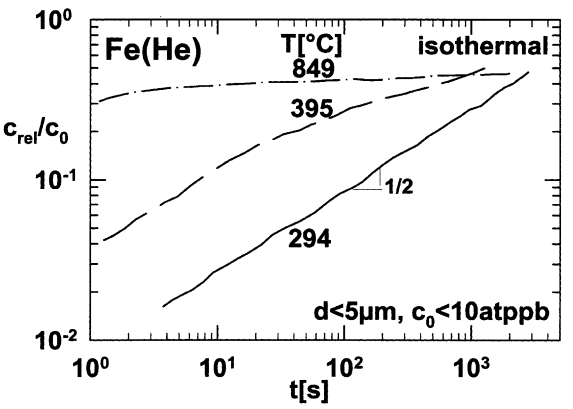

Fig. 5. He release from implanted iron during isothermal heating at the temperatures indicated. Specimen thickness and initial He concentration were below 5 μm and 10 at.ppb, respectively. A square root time dependence (slope 1/2) in this plot indicates diffusion [16].

4. Synergy effects

In nickel, austenitic stainless steels and some other fcc metals, effects of pre-implanted hydrogen or helium on retention or desorption of the other species were observed, see for example [17–19]. Detailed investigations on martensitic steels are in progress [9].

5. Effects of hydrogen and helium on microstructure and swelling

Results on the effect of hydrogen and helium on swelling are contradictory. In an early study, swelling of ferritic/martensitic steels under Cr-ion irradiation at 425–525°C to 100 dpa ($\Delta V/V \leqslant 0.15\%$) was not enhanced by the addition of 0.52 at.% H plus 0.13 at.% He [20]. On the other hand, recent investigations found an increase of void swelling in F82H at 400°C ($\leqslant 50$ dpa, $\Delta V/V \leqslant 1\%$) with increasing helium production as achieved by variation of neutron spectrum (HFIR vs. FFTF) or boron addition as summarised in Fig. 6 [21]. Further investigations are necessary to sort out possible effect of differences in dpa rate, as the higher rate in FFTF has been found to delay swelling [22].

6. Hardness and tensile properties

Fig. 7 shows changes of microhardness, measured at three temperatures in MANET-II and F82H specimens due to irradiation and hydrogen and/or helium implantation [23]. The data from instrumented hardness tests are plotted as a function of the concurrently produced displacement damage. The main results are: (1) within experimental error no difference in hardening of both materials; (2) virtually identical hardening at room temperature for specimens which were implanted with H and/or He and specimens which were only irradiated but not implanted (crosses); (3) on the other hand at −150°C (triangles down) and +170°C (triangles up) hardening of the implanted specimens is significantly higher, respectively, lower than that of specimens irradiated without implantation; (4) no significant difference between specimens implanted with H or He when compared on dpa basis. Correspondingly there are no additional synergy effects caused by H + He implantations.

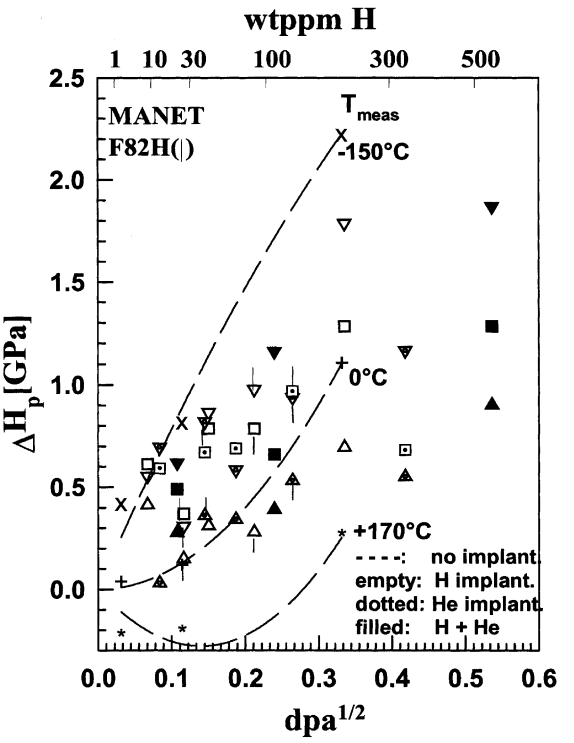

Fig. 7. Hardness of irradiated and H or He implanted MANET-II. Results for F82H are indicated by dashed symbols. Data are given for hardness measurements at −150°C (triangles down), 0°C (squares) and +170°C (triangles up) [23].

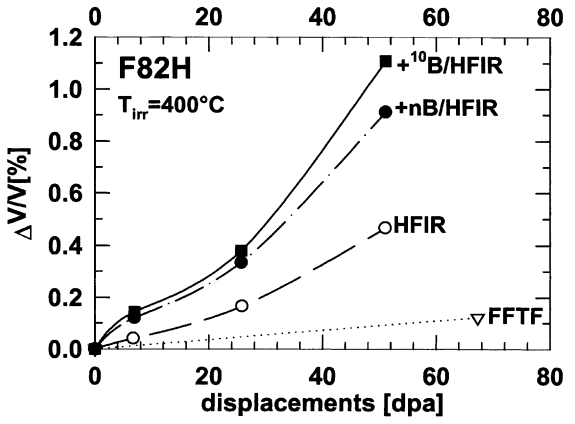

Fig. 6. Void swelling of F82H at 400°C as a function of displacement dose. The different reactors (FFTF or HFIR) and doping with boron give different helium production in the material [21].

Fig. 8 shows changes of micro- and nanohardness of MANET-II measured at room temperature after H and He single beam implantation as well as after Fe + He dual beam irradiation [24]. Included are results where the displacement damage and H and He production are caused by an 800 MeV proton beam. These data also indicate that hardening by H and He implantation is mainly produced by the concurrent displacement damage, at least up to He concentrations of about 0.5 at.%. Above this limit, possibly peculiar contributions from helium occur, probably due to bubble formation [25].

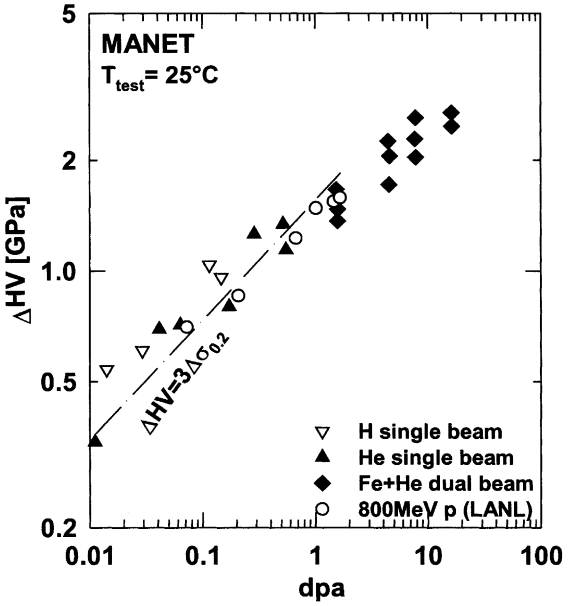

Fig. 8. Microhardness of MANET-II implanted by H, He and irradiated by dual beams of Fe and He, measured at room temperature. Included are results from 800 MeV proton irradiation at LANL [24].

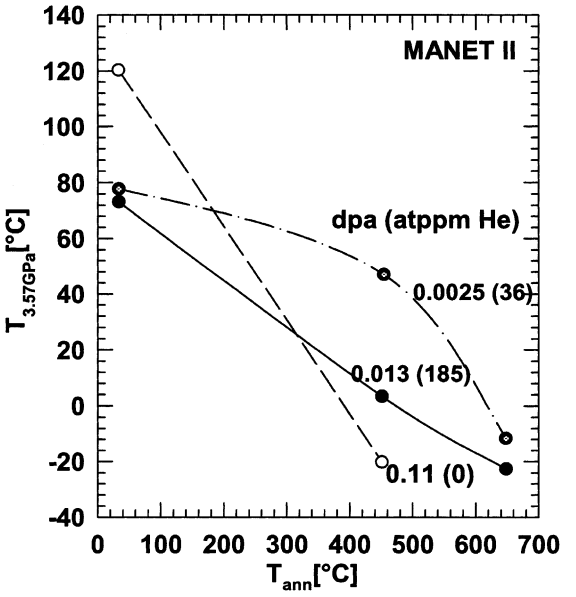

Fig. 9. Recovery of hardness of MANET-II irradiated and implanted to different displacement doses and helium contents. Instead of plotting hardness at a certain temperature, that temperature is given at which hardness reaches the value (3.57 GPa) which corresponds to the DBTT temperature of the virgin material [26].

The effect of implanted helium on the recovery of hardness is shown in Fig. 9 [26]. The figure gives a horizontal cut through hardness versus temperature curves like those in Fig. 7 and shows that helium causes retention of hardening to higher temperatures. More detailed investigations are needed to clarify the synergy effect of displacement damage and helium.

While martensitic stainless steels showed no change of tensile properties after implantation of 100 at.ppm helium at room temperature [27], higher concentrations of 350 [28] and 500 [29] at.ppm gave some increase in yield and ultimate tensile stress and reduction of uniform and total elongation, at least up to testing temperatures of ≈350°C. Implantation at 250°C to a concentration of 5000 at.ppm results in complete loss of ductility, while after implantation at 550°C some ductility is retained [30].

The effect of hydrogen on tensile properties of F82H is shown in Figs. 10 and 11. Yield stress and σ_{UTS} of the ≈380 μm thick specimens decrease strongly with implanted concentration when tested at room temperature, while at 200°C only a small effect and at 350°C almost no effect is observed. Uniform elongation ϵ_U as well as ϵ_f show a large decrease for testing at room temperature and much less at the higher temperatures [31]. These results may be compared to results after displacive damage production in reactors, which has a negligible effect at these low doses [32]. This indicates that

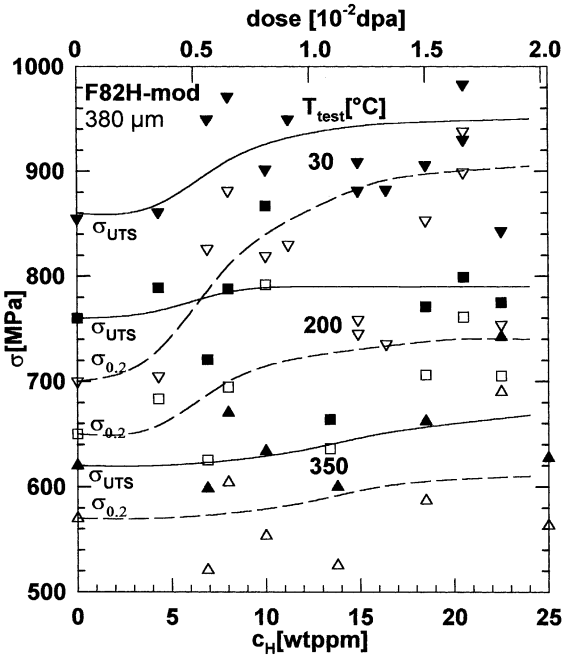

Fig. 10. Yield stress and ultimate tensile strength of F82H steel as a function of implanted hydrogen concentration from tensile tests performed at room temperature, 200°C and 350°C at strain rates around 1×10^{-4} s^{-1} [31].

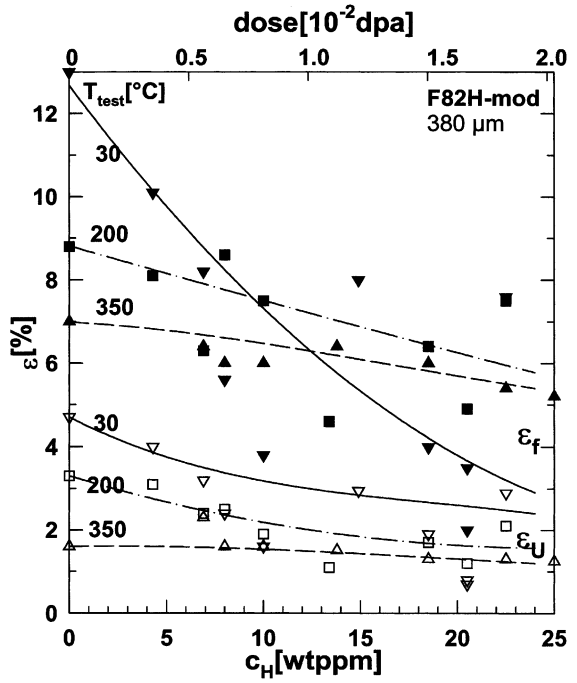

Fig. 11. Uniform and total elongation of F82H steel as a function of implanted hydrogen concentration from tensile tests performed at room temperature, 200°C and 350°C at strain rates around 1×10^{-4} s^{-1} [31].

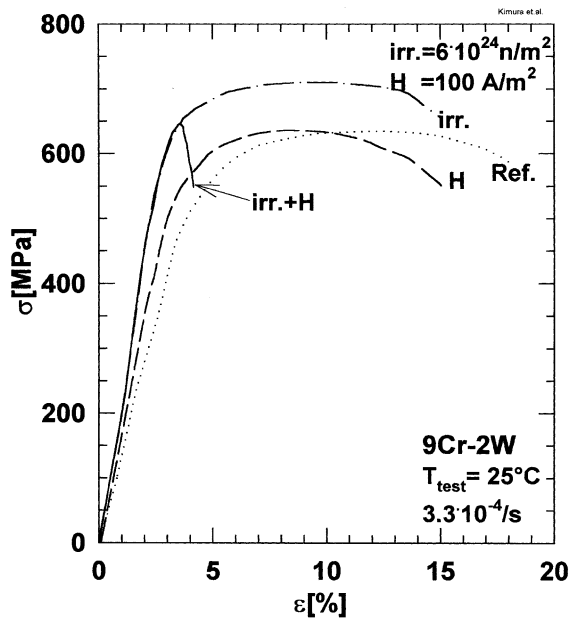

Fig. 12. Tensile curves of a 9Cr–2W steel in virgin state, after irradiation to 6×10^{24} n/m^2, after electrochemically loading with hydrogen, and after irradiation plus loading [33].

especially the strong loss in ductility must be ascribed to the presence of hydrogen.

Synergy effects of hydrogen plus irradiation have been studied by comparing tensile curves after reactor irradiation, electrochemical loading with hydrogen and loading of pre-irradiated specimens [33]. As can be seen from Fig. 12, irradiation or loading with H alone have minor effects, while loading of pre-irradiated specimens causes strong embrittlement.

7. Fracture and impact properties

In some basic studies of stress–strain curves, strong embrittlement of iron was found when it was loaded at cryogenic temperatures with low-energy helium [34]. Later investigations on low-activation martensitic steels, employing irradiation by dual beam or reactors in different spectra and/or of boron-doped material indicated effects of helium on fracture and impact properties. For example DBTT of F82H was increased by about 18°C after irradiation to a dose of 0.2 dpa in HFR, while the addition of 300 at.ppm He raises ΔDBTT by 44°C. At present the results are not detailed enough to clearly separate the effect of displacement damage and helium content. In Figs. 13 and 14 three-dimensional plots are given for 7–9% Cr and 12% Cr steels, respectively. From the limited amount of data it seems that both, displacement damage and helium contribute to ΔDBTT [14,15,35]. Further investigations are needed to determine the dose dependence of both effects more precisely and how both influences superimpose.

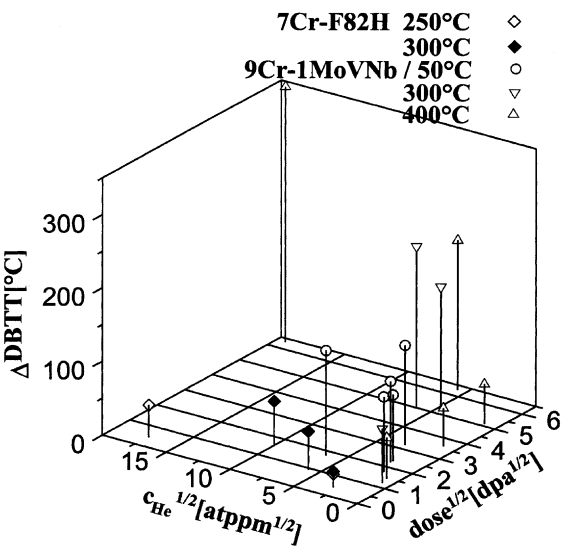

Fig. 13. Increase of DBTT of 7–9Cr-steels as a function of displacement dose and helium concentration [14,15,35].

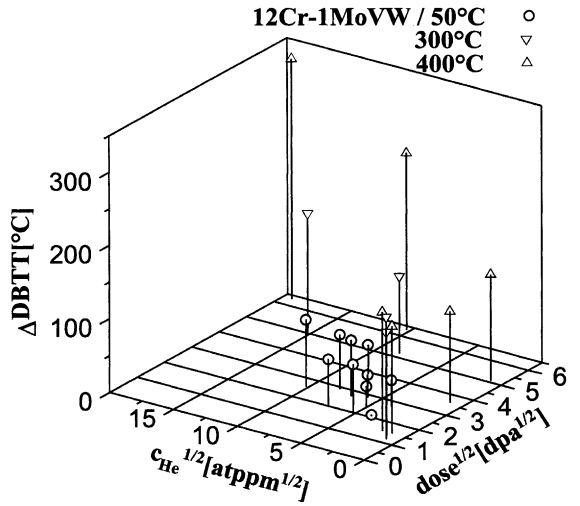

Fig. 14. Increase of DBTT of 12% Cr steels as a function of displacement dose and helium concentration [14,15,35].

8. Creep rupture and fatigue

One of the major advantages of ferritic/martensitic steels in comparison to austenitic steels is their resistance to high temperature helium embrittlement. This was revealed by in-beam creep rupture tests as shown in Figs. 15 and 16 [36]. In these experiments, helium is implanted at elevated temperatures under simultaneous application of a constant tensile stress. While austenitic AISI316L suffers a strong reduction in rupture time as well as rupture strain by the presence of helium, the detoriation is reduced in Ti-stabilised DIN1.4970, and virtually no effect of helium is observed in the martensitic steel DIN1.4914.

The effect of hydrogen on crack growth under cyclic loading was investigated in a 12Cr–1Mo steel [37]. In Fig. 17, the effect of frequency on the enhancement of crack growth rate by hydrogen is shown. The stronger effect at low frequencies is ascribed to the longer time available for hydrogen to reach the high stress areas ahead of crack tips. Also the reduction of fatigue life of MANET by hydrogen is enhanced at low frequencies and even more by additional holding times as shown in Fig. 18 [38].

Also the reduction of fatigue lifetime of austenitic steels by implanted helium is strongest at low frequencies [39]. In martensitic MANET-I, irradiated with 104 MeV α-particles to 1.6 dpa at 420°C and intermittently implanted to 400 at.ppm He, irradiation induced hardening and reduction of fatigue life was observed in post-irradiation fatigue testing [40]. On the other hand, much less degradation was observed when testing was performed during irradiation/implantation. Practically the same behaviour was observed in MANET-II, irradiated

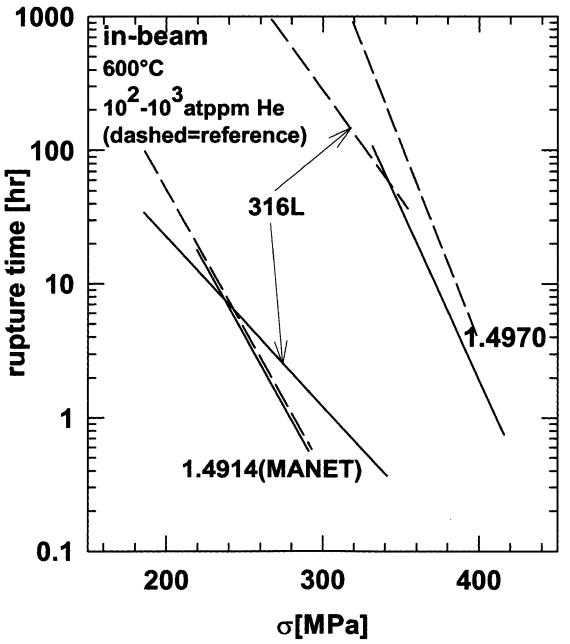

Fig. 15. Creep rupture time of virgin (dashed) and helium-loaded (solid) austenitic AISI316L, Ti-stabilised DIN1.4970 and martensitic DIN1.4914 steels. The helium was implanted at 600°C during simultaneous application of tensile stress [36].

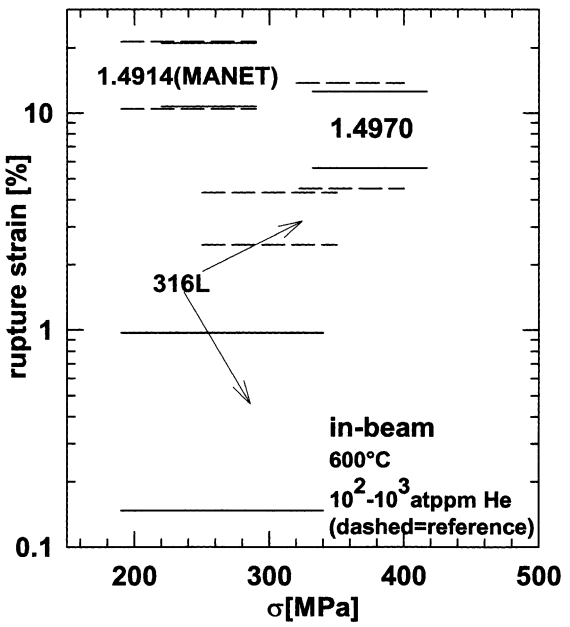

Fig. 16. Creep rupture strain of austenitic AISI316L, Ti-stabilised DIN1.4970 and martensitic DIN1.4914 steels. The helium (10^2–10^3 at.ppm, depending on lifetime) was implanted at 600°C during simultaneous application of tensile stress ('in-beam') [36]. Each pair of horizontal lines indicates the scatter-band of data from virgin (dashed) and helium-loaded (solid) specimens, respectively.

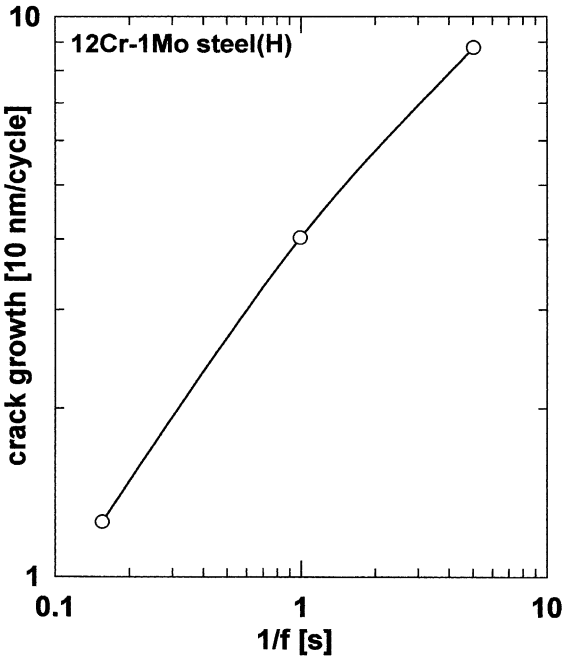

Fig. 17. Increase of crack growth rate by hydrogen as a function of inverse frequency in a 12Cr–1Mo steel at $\Delta K = 14$ MPa$\sqrt{}$m [37].

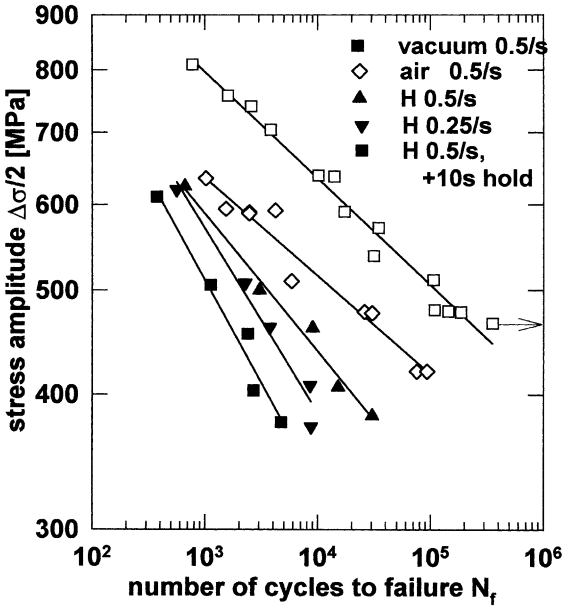

Fig. 18. Fatigue life of MANET at 295 K in vacuum, air and hydrogen under conditions as indicated [38].

with 590 MeV protons to around 0.2 dpa (corresponding to a production of 35 at.ppm He by transmutation [1]) for irradiation and testing at 300°C [41]. Investigations in the ESS relevant regime of lower temperatures are still missing.

9. Summary and conclusions

1. Hydrogen is effectively retained in martensitic stainless steels even at elevated temperatures due to trapping.
2. Helium is practically immobile even at elevated temperatures and therefore is quantitatively retained under ESS and ADS conditions.
3. Hardness is increased by hydrogen and helium implantation. At least the effect at room temperature can be quantitatively ascribed to the concurrently produced displacement damage.
4. Ductility is reduced by hydrogen at least up to about 300°C.
5. Helium contributes to embrittlement under impact conditions already at concentrations in the 100 at.ppm range, while tensile properties are significantly affected only at higher concentrations.
6. Helium implantation at elevated temperatures has only a minor effect on in situ creep rupture and fatigue properties, at least up to concentrations around 1000 at.ppm.

References

[1] S.L. Green, W.V. Green, F.H. Hegedues, M. Victoria, W.S. Sommer, B.M. Oliver, J. Nucl. Mater. 155–157 (1988) 1350.
[2] P. Jung, J. Nucl. Mater. 144 (1987) 43.
[3] D. Filges, R.-D. Neef, H. Schaal, in: Proceedings of International Workshop on Spallation Materials Technology, Oak Ridge, TN, 1996, p. 3.5.
[4] M.S. Wechsler, in: Proceedings of International Workshop on Spallation Materials Technology, Oak Ridge, TN, 1996, p. 3.5.
[5] D.S. Gelles, G.L. Hankin, M.L. Hamilton, J. Nucl. Mater. 251 (1997) 188.
[6] P. Jung, Fus. Technol. 33 (1998) 63.
[7] H. Rauh, H. Ullmaier, Report ESS 98-79-T, November 1998.
[8] G.V. Kidson, Landolt-Börnstein New Series, vol. III/26, Springer, Berlin, 1991, p. 504.
[9] C. Liu, P. Jung, to be published.
[10] F. Schliefer, C. Liu, P. Jung, J. Nucl. Mater. 283–287 (2000) 540.
[11] F. Wedig, P. Jung, J. Nucl. Mater. 245 (1997) 138.
[12] Data compiled by G. Alefeld, J. Völkl (Eds.), Hydrogen in Metals I, Springer, Berlin, 1978.
[13] P. Batfalsky, H. Schroeder, J. Nucl. Mater. 122&123 (1984) 1475.
[14] R.L. Klueh, D.J. Alexander, J. Nucl. Mater. 218 (1995) 151.
[15] R. Lindau, A. Möslang, D. Preininger, M. Rieth, H.D. Röhrig, J. Nucl. Mater. 271&272 (1999) 450.

[16] R. Vassen, H. Trinkaus, P. Jung, Phys. Rev. B 44 (1991-I) 4206.
[17] K.L. Wilson, M.I. Baskes, J. Nucl. Mater. 76&77 (1978) 291.
[18] E. Abramov, J. Nucl. Mater. 212–215 (1994) 1384.
[19] J.D. Hunn, M.B. Lewis, E.H. Lee, in: Proceedings of Second International Topical Meeting on Nuclear Application of Accelerator Technology, Gatlinburg, September 20–23, 1998, ANS, 1998, p. 375.
[20] D.J. Mazey, G.P. Walters, S.N. Buckley, S.M. Murphy, W. Hanks, D.E.J. Bolster, J. Nucl. Mater. 155–157 (1988) 891.
[21] E. Wakai, N. Hashimoto, Y. Miwa, J.P. Robertson, R.L. Kliueh, K. Shiba, S. Jitsukawa, J. Nucl. Mater. 283–287 (2000) 799.
[22] B.H. Sencer, F.A. Garner, J. Nucl. Mater. 283–287 (2000) 164.
[23] P. Jung, J. Nucl. Mater. 258–263 (1998) 124.
[24] H. Ullmaier, E. Camus, J. Nucl. Mater. 251 (1997) 262.
[25] J.D. Hunn, E.H. Lee, T.S. Byun, L.K. Mansur, J. Nucl. Mater. 282 (2000) 131.
[26] P. Jung, J. Chen, in: P. Jung, H. Ullmaier (Eds.), Proceedings of the IEA International Symposium on Miniaturized Specimens for Testing of Irradiated Materials, Jülich, 1995, p. 85.
[27] U. Stamm, PhD thesis, RWTH Aachen 1988, Report KFA Jülich, Jül-2225, August 1988.
[28] A. Möslang, D. Preininger, J. Nucl. Mater. 155–157 (1988) 1064.
[29] K.K. Bae, K. Ehrlich, A. Möslang, J. Nucl. Mater. 191–194 (1992) 105.
[30] J. Henry, P. Jung, to be published.
[31] P. Jung, H. Klein, C. Liu, to be published.
[32] A. Alamo, et al., Presented at the Fifth Milestone Meeting on Data Base Evaluation, Brasimone, November 2000 (unpublished).
[33] A. Kimura, H. Kayano, M. Narui, J. Nucl. Mater. 179–181 (1991) 737.
[34] K. Shinohara, Y. Nakamura, S. Kitajima, M. Kutsuwada, M. Kaneko, J. Nucl. Mater. 155–157 (1988) 1154.
[35] M. Rieth, B. Dafferner, H.D. Röhrig, J. Nucl. Mater. 233–237 (1996) 351.
[36] H. Schroeder, U. Stamm, ASTM STP 1046 (1989) 223.
[37] G.F. Rodney, R.H. Jones, J. Nucl. Mater. 155–157 (1988) 760.
[38] J.I. Shakib, H. Ullmaier, E.A. Little, R.G. Faulkner, W. Schmitz, T.E. Chung, J. Nucl. Mater. 212–215 (1994) 579.
[39] L.S. Batra, H. Ullmaier, K. Sonnenberg, J. Nucl. Mater. 116 (1983) 136.
[40] R. Lindau, A. Möslang, J. Nucl. Mater. 212–215 (1994) 594.
[41] P. Marmy, J. Nucl. Mater. 212–215 (1994) 594.